2014 UKSim-AMSS 8th European Modelling Symposium

Decentralized Feedback Design for a Compliant Robot Arm

Houman Dallali, Gustavo Medrano-Cerda, Navvab Kashiri, Nikos Tsagarakis and Darwin Caldwell
Department of Advanced Robotics,Fondazione Istituto Italiano di Tecnologia (IIT), Genova 16163, Italy
{houman.dallali, gustavo.cerda, navvab.kashiri, nikos.tsagarakis, darwin.caldwell}@iit.it

***Abstract*—Enhancing safety during interaction with environment and improved force control has led to design of highly compliant robotic arms. However, due to introduction of passive compliance in series with actuators the links' interactions and coupling effects become much more important. In this paper a direct decentralized approach for designing PD-PID gains, given the dynamic multivariable model of the compliant robot arm, is proposed. The proposed method is based on Linear Matrix Inequality (LMI) formulation with full state feedback in discrete time that automatically designs the decentralized gains for all the four joints of the robot in one shot. Experimental results for a four Degree of Freedom (DoF) compliant robot arm are provided to illustrate the effectiveness of this method.**

Keywords–control of highly compliant joints; LMI; LQR; decentralized state feedback;

I. Introduction

Conventional robot arms that are used in structured environments such as factories use rigid joints, controlled with high gain PID controllers, which lead to high mechanical impedance. These robot arms are often placed inside cages to avoid injuries to the human workers who are in vicinity of these robots. In recent years, new applications have been realized to use low mechanical impedance and safe robot arms in unstructured environments such as houses or public places. These robots use passive elasticity to decouple the actuator inertia from the load and provide a low impedance system with improved force control characteristics. However, introduction of series elasticity in the robot joints requires more advanced control methods to deal with increased coupling effects between the joints.

Most robot arms with rigid joints implement independent PD or PID joint controllers for trajectory tracking. This works well due to highly stiff joints and high gear ratios which reduces the coupling effect between the joints [1]. In independent joint controller design, each joint of the robot is treated as an independent subsystem and the interactions and coupling effects between the joints are treated as unknown disturbances that must be rejected by the independent joint controller [1]. However, the idea of decentralized full state feedback design is to include these known couplings and interactions in the state feedback design via an optimization problem, in order to assist the natural motion of the robot rather than to fight against the known link's interactions.

Several control methods based on feedback linearization [2] and the theory of integral manifold [3] have been proposed for controlling flexible joint robots. However, these schemes are complex from an implementation point of view and require a precise knowledge of the robot's dynamic parameters to achieve stability and a good performance in practice. On the contrary, in [4] a simple PD controller with gravity compensation was proved to stabilize flexible joint robots about a reference position. The PD feedback controller was introduced on the motor's position and velocity. The position of the link was shown to be sensitive to uncertainties in gravitational and elastic parameters, since the link position was controlled indirectly via the motor position without direct feedback or integral action on the link position.

In [5], a full state feedback controller was proposed which utilized both the motor and link states to achieve a better performance compared to simple PD controller introduced in [4] and still keep the controller simple for implementation. The implementation problems of the complex control schemes were pointed out as the motivation for the full state feedback method. However, the full state feedback design was based on independent joint control and the dynamic links' interactions were not considered. A comparison between use of decentralized and centralized controllers is provided in [6]. Therefore, the problem is how to tune the full state decentralized feedback gains by directly taking the joint's elasticity and multibody interactions into account.

LMI provide a powerful tool for designing the state feedback with decentralized structure. LMI based decentralized PID design has been widely studied in the control engineering literature, [7]–[11]. In addition, the Linear Quadratic Regulator (LQR) formulation of the feedback design is desired since choosing pole locations for a complex system such as a humanoid is a challenging task and LQR formulation is proved to have excellent robustness against parameter variations [12]. Hence, a discrete time LMI-LQR decentralized feedback design approach for compliant robot arms is proposed in this paper to design full state feedback designs. It is shown in section III that the feedback takes the form of a PID control on motor side and a PD on the link side of the robot arm joints.

This paper is organized as following. In section II the mechanical model of CompAct^{TM} arm is explained. In section III the discrete time LQR based feedback formulation is given in terms of the corresponding LMIs and

978-1-4799-7412-2/14 $31.00 © 2014 IEEE
DOI 10.1109/EMS.2014.101

the decentralized feedback structure is discussed. In section IV experimental results of the 4 DoF CompAct™ arm are provided to illustrate the effectiveness of this method. Finally the conclusion and future work are discussed.

II. MODELLING

In this section, modelling of the CompAct™ arm is presented. The CompAct™ arm has 4 DoF including 3 DoF for the shoulder and one for the elbow. The shoulder DoFs consist of extension-flexion, adduction-abduction and humeral-roll degrees of freedom, respectively from joint one to joint three and an additional DOF for the implementation of the elbow flexion-extension motion as the fourth joint of the arm. All joints have passive compliance in series with brushless DC motors. These actuators are controlled with a dedicated DSP board, which are connected to a computer running real-time Linux operating system. The model includes the mechanical equations of motion are linearized about the home posture as shown in Fig.1 and coupled to actuator dynamics via the passive compliant elements. The model is represented in state space and integrator dynamics are introduced in the augmented plant for reference tracking.

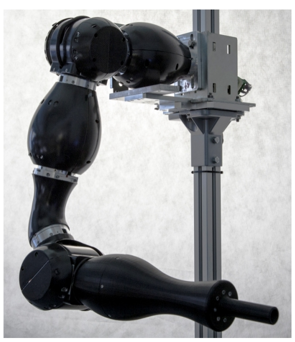

Figure 1. The CompAct™ Arm, [13].

A. Mechanical Model

The model is derived in symbolic form using Robotran [14] that is a general dynamic Matlab based multi-body modelling software, using the method explained in [15]. The CompAct™ arm model is:

$$M(\mathbf{q})\ddot{\mathbf{q}} + C(\mathbf{q}, \dot{\mathbf{q}})\dot{\mathbf{q}} + G(\mathbf{q}) = \tau(\mathbf{q}, \dot{\mathbf{q}}, \mathbf{q}_m, \dot{\mathbf{q}}_m), \qquad (1)$$

where $\mathbf{q}$ is the angular joint positions in relative coordinates, $M(\mathbf{q})$ is the mass-inertia matrix which is a function of the joint angles and $C(\mathbf{q}, \dot{\mathbf{q}})$ is the vector of coriolis forces and $G(\mathbf{q})$ represents gravitational forces and is a function of joint angles. τ is a vector of torques applied to the links. $\mathbf{q_m}$ and $\dot{\mathbf{q}}_\mathbf{m}$ are vectors of motor position and motor velocity, respectively. In the case of CompAct™ arm, due to passive compliance in the joints, the torque τ is a function of spring deflection that depends on the motor and link position and velocity. Hence the torque provided by the actuator dynamic equation is discussed in the next section.

B. Actuator Dynamics

The main purpose of including actuator dynamics is two fold. The first is to include the brushless electric motor inertia that when reflected to the output of gearbox has the same order of magnitude as the link inertia. The second is that the electric motors are connected in series with a compliant element to store and release energy during walking. Therefore the links are indirectly driven by torque provided by the spring deflections. The mechanical diagram of a single compliant joint is shown in Fig. 2. The input to the joint T_m (the motor torque) is proportional to the motor's current. The current can be also expressed as a gain times the voltage minus a damping term due to the back EMF. The linear equation that describes the overall relationship between the applied voltage and the joint motion is:

$$J\ddot{\mathbf{q}}_m + D_m\dot{\mathbf{q}}_m = V_m\ \mathbf{u} - \tau(\mathbf{q}, \dot{\mathbf{q}}, \mathbf{q}_m, \dot{\mathbf{q}}_m), \qquad (2)$$

where J is the reflected motor inertia matrix with diagonal elements being J_m, D_m is the total (including the back EMF damping) reflected motor damping matrix with diagonal elements being d_m as shown in Fig. 2, V_m is the voltage to torque gain matrix, $\mathbf{u}$ is the vector of motors' voltages. The mechanical torque τ is shown to be a function of the motor and link position and velocity, i.e.

$$\tau(\mathbf{q}, \dot{\mathbf{q}}, \mathbf{q}_m, \dot{\mathbf{q}}_m) = K_s(\mathbf{q}_m - \mathbf{q}) + D_s(\dot{\mathbf{q}}_m - \dot{\mathbf{q}}), \qquad (3)$$

where K_s and D_s are the joint stiffness and damping diagonal matrices. Each element on the diagonal of K_s is the passive stiffness k_s and each element on the diagonal of D_s is the damping in parallel to the passive stiffness d_s, as shown in Fig. 2. Further modelling details are provided in [16]. In order to formulate the control design problem as a set of LMIs these equations are formulated in state space form in the next section.

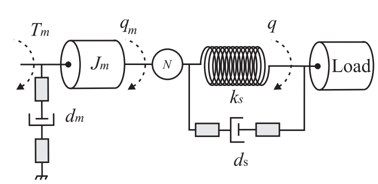

Figure 2. Mechanical diagram of a compliant joint driving a load inertia. N represents the gearbox reduction ratio.

C. Linear Discrete-Time State Space Models

The coupled linearized mechanical model and the actuator dynamics are discretized and represented in state space as:

$$\tilde{\mathbf{x}}(k+1) = F\tilde{\mathbf{x}}(k) + H\mathbf{u}(k), \qquad (4)$$

where the state $\tilde{\mathbf{x}} = [\mathbf{q}, \dot{\mathbf{q}}, \mathbf{q}_m, \dot{\mathbf{q}}_m]^T$, $\mathbf{u}$ is the applied control signal, F is discretized state matrix and H is the discretized input matrix. Moreover, the final goal of the inner loop feedback is to track the desired trajectories in face of noise and disturbances. Hence an auxiliary integrator is introduced as:

$$\mathbf{z}(k+1) - \mathbf{z}(k) = \mathbf{r}(k) - E\tilde{\mathbf{x}}, \tag{5}$$

where $\mathbf{z}$ is the discrete time integrator state and $\mathbf{r}$ is the motor's reference position. Hence the augmented system is:

$$\mathbf{x}(k+1) = A\mathbf{x}(k) + B\mathbf{u}(k) + B_r\mathbf{r}(k), \tag{6}$$

where $\mathbf{x} = [\tilde{\mathbf{x}}, \mathbf{z}]^T$, $A = \begin{bmatrix} F & 0 \\ -E & I \end{bmatrix}$, $B = \begin{bmatrix} H \\ 0 \end{bmatrix}$, $E = [0 \quad I]$ and $B_r = \begin{bmatrix} 0 & I \end{bmatrix}^T$, where E measures the motor positions, with 0 and I being the zero matrix and identity matrix of suitable dimension.

It should be noted that the joint variables are ordered as joint positions, joint velocities, motor positions, motor velocities and integrators. However, for convenience in the definition of LMI variables, a permutation matrix is used to reorder the states as $[q_i, \dot{q}_i, q_{mi}, \dot{q}_{mi}, z_i]^T$ for each joint, where i represents the joint index.

III. CONTROL DESIGN

In this section, the discrete time formulation of the LQR based PID design is explained via LMIs. The linear discrete time system (6) is utilized with zero reference input to design the PID joint servo controller. Once the feedback gain is designed, the desired reference positions $\mathbf{r}$ are tracked via B_r the second input matrix.

A. LMI Formulation

The LMI formulation is considered in two parts. The first part represents the stability of the stochastic linear system in terms of the state covariance matrix and the corresponding Lyapunov equation. Then the quadratic LQR performance index is presented to formulate the optimal feedback gain as the solution to the LMI convex optimization problem.

Let the discrete time system with noise be described by:

$$\mathbf{x}(k+1) = A\mathbf{x}(k) + B\mathbf{u}(k) + \eta, \tag{7}$$

where η is noise. Assuming that the state $\mathbf{x}$ is available for measurement and the pair (A, B) is controllable, the feedback can be expressed as $\mathbf{u}(k) = -K\mathbf{x}(k)$ and the closed loop system is:

$$\mathbf{x}(k+1) = (A - BK)\mathbf{x}(k) + \eta, \tag{8}$$

where $(A-BK)$ is asymptotically stable. The main purpose of this section is to impose a block diagonal structure on the feedback gain matrix as:

$$K = \begin{bmatrix} K_1 & 0 & 0 & \cdots & 0 \\ 0 & K_2 & 0 & \cdots & 0 \\ 0 & 0 & \ddots & \cdots & 0 \\ \vdots & \vdots & \cdots & K_{n-1} & 0 \\ 0 & 0 & \cdots & 0 & K_n \end{bmatrix}, \tag{9}$$

where the K_i blocks are row vectors of dimension 1 by 5 and n is the number of joints. Each block in (9) contains the five PD-PID gains such that

$$K_i = [K_p,\ K_d,\ K_{pm},\ K_{dm},\ K_z], \tag{10}$$

where K_p and K_d are the feedback from the link position and velocity, K_{pm} and K_{dm} are feedback from motor position and velocity, and K_z is feedback from the discrete integrator states. The steady-state state covariance matrix $P = E[\mathbf{x}\mathbf{x}^T]$ is the solution to Lyapunov equation

$$P - (A - BK)P(A - BK)^T - \hat{Q} = 0, \tag{11}$$

where the noise covariance matrix is $E[\eta\eta^T] = \hat{Q}$. If every entry in the noise vector has the same variance β and the entries are all statistically independent or uncorrelated then the noise covariance is $E[\eta\eta^T] = \beta I$. Hence,

$$P - \beta I - (A - BK)P(A - BK)^T > 0. \tag{12}$$

Since this inequality is nonlinear in K and P, a change of variable is necessary. Equation (12) can be written as

$$P - \beta I - (AP - BY)P^{-1}(AP - BY)^T > 0, \tag{13}$$

where $Y = KP$. Equation (13) can be expressed as the Schur complement of P:

$$\begin{bmatrix} (P - \beta I) & (AP - BY)/\delta \\ (AP - BY)^T/\delta & P \end{bmatrix} > 0, \tag{14}$$

where δ is the radius for the circular LMI region which constrains the closed loop eigenvalues. In practice $0.8 \leq \delta \leq 1$. The above LMI equation represents all feedback gains K that stabilize the linear system. In order to find the optimum gain the LQR quadratic cost function in terms of the penalized state and control input is derived as in [17].

$$\mathbf{y}(k) = \begin{bmatrix} Q^{\frac{1}{2}} & 0 \\ 0 & R^{\frac{1}{2}} \end{bmatrix} \begin{bmatrix} \tilde{\mathbf{x}}(k) \\ \mathbf{u}(k) \end{bmatrix} = \begin{bmatrix} Q^{\frac{1}{2}} \\ -R^{\frac{1}{2}}K \end{bmatrix} \mathbf{x}(k), \tag{15}$$

where $Q = Q^T \geq 0$ and $R = R^T > 0$. Then the LQR cost function can be defined as

$$J = E[tr[\mathbf{y}^T\mathbf{y}]] = E[tr[\mathbf{y}\mathbf{y}^T]], \tag{16}$$

where $tr[\,]$ denotes trace of a matrix. The simplified cost function in terms of the LQR penalty matrices is

$$J = tr[QP] + tr[R^{\frac{1}{2}} K P K^T R^{\frac{1}{2}}]. \quad (17)$$

However, the second term of the cost above is nonlinear in K and P and must be redefined for LMI representation. Let

$$X = R^{\frac{1}{2}} K P K^T R^{\frac{1}{2}}, \quad (18)$$

where X is a symmetric LMI variable. Equation (18) can be written as a Schur complement:

$$\begin{bmatrix} X & R^{\frac{1}{2}} Y \\ Y^T R^{\frac{1}{2}} & P \end{bmatrix} > 0, \quad (19)$$

The LMI optimization problem can be written as

$$\min_{(P,Y,X)} \quad tr[QP] + tr[X], \quad (20)$$

subject to (14) and (19). The centralized feedback is obtained by

$$K = YP^{-1}. \quad (21)$$

In general, the feedback gain in (21) has a centralized structure. That is the feedback for each joint depends on states of other joints. The centralized feedback requires all the arm dynamic information to be available in one location (for instance a central computer) to perform the calculations. In fact, without imposing constraints on K the solution of (20) subject to (14) and (19) is the same as the discrete time LQR solution. However, for practical implementation on joint DSP controllers, it is often desired to have decentralized structure. This is because each actuator is controlled by a separate DSP controller performing the feedback control, locally.

The decentralized structure on the feedback gain K as in (9) can be realized by imposing a block diagonal structure on the LMI variables P and Y. It can be easily shown that if these variables have a block diagonal structure the resulting feedback gain in (21) will have the decentralized structure. Hence in this paper, P and Y are defined to have similar structure as in (9). The only difference is that diagonal blocks of P are square matrices of dimension 5 and diagonal blocks of Y have the same dimension as blocks of K. The next section demonstrates experimental results of this method on the CompAct™ robot arm.

IV. EXPERIMENTAL VALIDATION

This section is organized in three parts. Firstly, the experimental setup is explained in section IV-A. Secondly, the details about controller implementation are provided in section IV-B. Finally, the step and sine wave experimental results are reported in section IV-C.

A. Experimental Setup

In this section, the 4 DoF CompAct™ arm is used to validate the control design. Full multivariable mechanical model of the arm including actuator dynamics and passive compliance is used. The model is linearized about the home posture as shown in Fig. 1 which corresponds to zero angles, velocities and accelerations. The linearized model is discretized with 1 ms sampling time to derive the state space equations given in (6) and the LMI-LQR algorithm is used to design the decentralized feedback gains. The dynamic parameters of the robot such as the mass, centre of mass and inertias are obtained from the CAD software and DC motor data sheet.

In terms of sensors, there are two 12 bit position encoders to measure the motor and link angles. The motor encoder is placed before the gearbox with gear ratio of 100:1, and therefore gives 100 times better signal for the motor position when reflected to the output of the gearbox. In order to obtain the velocity signal a third order Butterworth differentiator filter with cut off frequency of 20 hertz is used. This cut off frequency was chosen in several experimental tests to reduce the spikes on the velocity signal specially during slow motions. Hence all state variables are available for the state feedback control. The size of the state vector is 20×1 which includes 4 link positions, 4 link velocities, 4 motor positions, 4 motor velocities and 4 integrators introduced on the link positions, respectively. The same ordering is maintained in the LQR state and input penalty matrices Q and R used in section IV-B to provide an intuitive way of tuning the controllers. The passive compliance in the shoulder extension-flexion and adduction-abduction is 188 Nm/rad and the compliance in shoulder roll and elbow flexion-extension is 103 Nm/rad, respectively.

B. Controller Implementation

The LQR state and input penalties in the original coordinates are $Q = \text{diag}\{10 \times Q_1,\ 0.1 \times Q_2,\ 10 \times Q_3,\ 0.1 \times Q_4,\ 0.5 \times Q_5\}$, where $Q_1 = [1, 1, 1, 0.1]$, $Q_2,\ Q_3,\ Q4,\ Q5$ are $[1, 1, 1, 1]$, and $R = \text{diag}\{2, 4, 4, 2\}$ and the input noise variance is $\beta = 0.01$, where p is the dimension of the state space that is 20 and n is 4. The size of the circular LMI region to constrain the closed loop poles is chosen as $\delta = 0.999990$ to relax the constraint on the size of eigenvalues. Increasing bandwidth was realized by reducing the input penalties and increasing the state penalties. δ provides an additional constraint and tuning parameter to obtain faster responses by directly imposing some values on the closed loop eigenvalues. The penalties and state space model are transformed using the permutation matrix as described in the previous section. In general, reducing the penalty R increases the speed of the response but also leads to larger control signals. Also, increasing the penalty on the integrators Q_5 increases the speed of the response by producing larger integral gains.

The LMI optimization has 90 decision variables which depends on the size of LMI variables $(Y,\ P,\ X)$ used in (20) and (21). The resulting gains are reported in Table I. The proportional gains K_p for link position and K_{pm} for motor position are in (V/rad), damping gains K_d for link velocity and K_{pm} for motor velocity are in (V.sec/rad) and integrator gains (accumulating the error between reference and motor position) are in (V/rad.sec). The resulting gains are shown in Table I. The controller formula for each joint is implemented as:

$$u_i = K_i \times [q_i, \dot{q}_i, q_{mi}, \dot{q}_{mi}, z_i]^T, \qquad (22)$$

with K_i defined in (10) for each joint.

TABLE I
DESIGNED FEEDBACK GAINS

Joint ID	K_p	K_d	K_{pm}	K_{dm}	K_z
1	-8.24	5.72	103.57	0.58	-0.5
2	-196.08	11.45	277.07	1.43	-0.34
3	-275.9	3.94	358.15	1.79	-0.34
4	-73.76	0.51	147.38	0.8	-0.49

C. Experimental Results

In order to characterize the performance of the designed tracking system, experimental step responses of each joint controlled by the decentralized gains are presented. The step tests for three shoulder joints and elbow are shown in Figs. 3, 4, 5 and 6, respectively. Size of the step is chosen to be 10 degrees (0.174 radian) to excite the dynamics but also avoid damaging the arm. The achieved bandwidth of the system is about 1 hertz and a major limitation in increasing the bandwidth further was the noisy velocity signals and use of filtering (used for velocity estimation) which introduces delay in the control system. In particular the effect of noisy link velocity signal can be observed on the generated control input signals for joints one and two as shown in Figs. 3 and 4. The actuators of the CompAct$^{\text{TM}}$ arm have a maximum input voltage of ± 24 volts which compared to the step control input shows the control is far from saturation. The effect of noisy velocity signal can be seen during the first 0.5 seconds in Fig. 3 when the joint is not moving but voltage spikes are produced due to the spikes in the link velocity estimates.

Furthermore, an overshoot of about 10% can be seen in the step response which is due a feedforward gain with value of 25% of the K_{pm} times the reference position is used in the experiments which should be adjusted to avoid this overshoot. In addition to step response experiments, sine tracking was also tested on the joints as shown in Fig. 7 for joint one. The reference signal for joints one, three and four is chosen as $r(t) = 10sin(6.28t)$ which has 1 hertz frequency with amplitude of 10 degrees. The reference signal for joint two due to mechanical limits is chosen as $r(t) = 10(1 - cos(6.28t))$. It should be noted that, the joint tracking can be still improved by formulating an output feedback problem to derive optimal decentralized feedback gains for sensors with cleaner signals. Hence, as a future work studying the output feedback control to only use the sensors which give better signals will be considered.

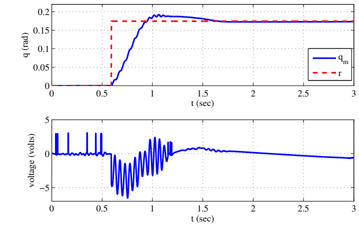

Figure 3. The step response of joint one, shoulder extension-flexion.

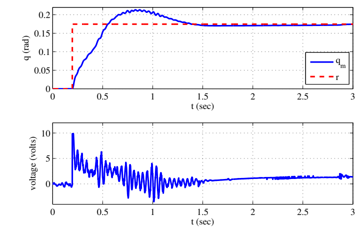

Figure 4. The step response of joint two, shoulder adduction-abduction.

V. CONCLUSION

The decentralized full state feedback design via LQR-LMI approach was presented in discrete time. It was shown

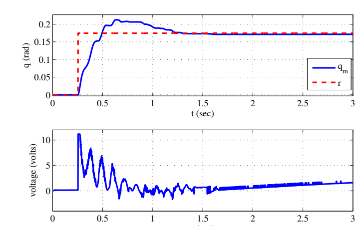

Figure 5. The step response of joint three, shoulder roll.

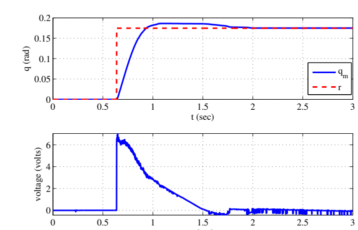

Figure 6. The step response of joint four, elbow.

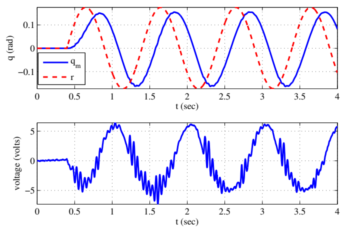

Figure 7. The sine response of joint one, shoulder extension-flexion.

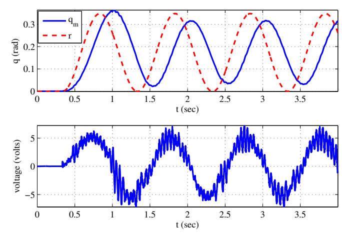

Figure 8. The cosine response of joint two, shoulder adduction-abduction.

that this method can be applied to compliant robots to design the servo controller with a decentralized structure. The compliant CompAct^{TM} robot arm with 4 DoF was chosen to illustrate the ideas experimentally. The LQR-LMI optimization problem showed promising results to design the PD-PID feedback gains with the desired bandwidth. Future work will focus on theoretical and experimental study of output feedback problem with feed-forward gravity compensation to improve the dynamic tracking of the robot arm in terms of bandwidth and utilization of sensors with

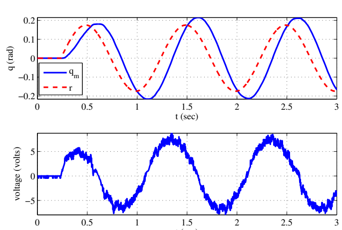

Figure 9. The sine response of joint three, shoulder roll.

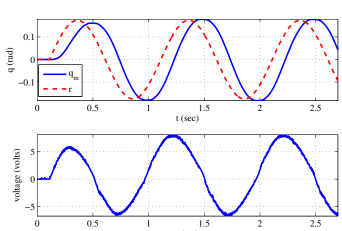

Figure 10. The sine response of joint four (elbow).

more cleaner (less noisy) signals in the control system. This method can be utilized in compliant robot arms to benefit from various sensor readings such as position and torque in the joint feedback.

Acknowledgment

This project was supported by the WALK-MAN (FP7-ICT 611832) & SAPHARI (FP7-ICT-2011-7) projects.

References

[1] M. W. Spong, S. Hutchinson and M. Vidyasagar, *Robot Modeling and Control*, John Wiley and Sons, Inc., 2006.

[2] M. W. Spong, "Modeling and control of elastic joint robots," ASME J. Dynam. Syst., Meas., Contr., Vol. 109, pp. 310-319, 1987.

[3] M. W. Spong, K. Khorasani, and P. V. Kokotovic, "An integral manifold approach to the feedback control of flexible joint robots," IEEE J. Robotics and Automation, Vol. RA-3, pp. 291-300, 1987.

[4] P. Tomei, "A Simple PD Controller for Robots with Elastic Joints", IEEE Tran. On Automatic Control, Vol. 36, No. 10, Oct. 1991.

[5] Alin Albu-Schaffer, Gerd Hirzinger, "State feedback controller for flexible joint robots: A globally stable approach implemented on DLRs light-weight robots," in Proc. IEEE/RSJ Int. Conf. on Intelligent Robots and Systems (IROS), 2000, pp. 1087-1093.

[6] H. Dallali, G. A Medrano-Cerda, M. Brown, "A comparison of multivariable & decentralized control strategies for robust humanoid walking", in Proc. of UKACC International Conference on Control 2010, Coventry, UK, 2010, pp 1-6.

[7] A. I. Zecevic, and D. D. Siljak, "Control design with arbitrary information structure constraints," Automatica, Vol. 44, No. 10, pp. 26422647, 2008.

[8] M. Saeki, "Fixed structure PID controller design for standard H_∞ control problem," Automatica, Vol. 42, pp. 93-100, 2006.

[9] D. Rosinov and V. Vesel, "Robust PID Decentralized Controller Design Using LMI," Int. Journal of Computers, Communications & Control, Vol. II, No. 2, pp. 195-204, 2007.

[10] L. El Ghaoui and V. Balakrishnan, "Synthesis of Fixed-Structure Controllers Via Numerical Optimization," in Proc. IEEE Conf. on Decision and Control, 1994, pp.2678 - 2683.

[11] L. Vandenberghe, V. Balakrishnan, "Algorithms and software for LMI problems in control," Control Systems, IEEE , Vol. 17, No. 5, pp. 89-95, Oct 1997.

[12] M. G. Safonov, M. Athans, "Gain and Phase Margin for Multiloop LQG regulators," IEEE Tran. On Automatic Control, Vol. AC-22, No. 2, Apr. 1977.

[13] N. Kashiri, M. Laffranchi, N. G. Tsagarakis, A. Margan, D. G Caldwell, "Physical Interaction Detection and Control of Compliant Manipulators Equipped with Friction Clutches", in Proc. IEEE International Conference on Robotics and Automation (ICRA), Hong Kong, 2014, pp. 1066-1071.

[14] J. Samin, and P. Fisette, *Symbolic modelling of multibody systems, Solid mechanics and its applications*, 1st ed., Kluwer Academic Publishers, 2003.

[15] H. Dallali, M. Mosadeghzad, G. A Medrano-Cerda, N. Docquier, P. Kormushev, N. Tsagarakis, Z. Li, D. Caldwell, "Development of a dynamic simulator for a compliant humanoid robot based on a symbolic multibody approach", in Proc. IEEE International Conference on Mechatronics (ICM), Vicenza, Italy, 2013, pp. 598-603.

[16] N. Kashiri, M. Laffranchi, N. G. Tsagarakis, I. Sardellitti, and D. G. Caldwell, "Dynamic Modeling and Adaptable Control of the CompAct Arm," in Proc. IEEE International Conference on Mechatronics, Vicenza, Italy, 2013, pp. 477-482.

[17] B. D. O. Anderson and J. B. Moore, *Optimal Control: Linear Quadratic Methods*, New Jersey, Prentice-Hall, 1998.

[18] J. C. Geromel, J. Bernussou, and P. L. Peres, "Decentralized Control Through Parameter Space Optimisation," Automatica, Vol. 30, No. 10, pp. 1565-1578, 1994.